RESEARCH ARTICLE

Improving the bioavailability of cinnamaldehyde hydroxypropyl based on β-cyclodextrin inclusion technology

Xiaoying Fu, Yan Jiao, Yuanyuan Zhang*

Cangzhou Medical College, Cangzhou, Hebei, China.

Received: January 6, 2026; **accepted:** May 8, 2026.

Cinnamaldehyde, a natural aromatic compound derived from cinnamon, has attracted considerable attention due to its antioxidant, antibacterial, and preservative properties and has been widely applied in food preservation, pharmaceutical formulations, and functional health products. However, its poor water solubility, volatility, and instability in aqueous environments significantly restrict its practical utilization. The application of natural active ingredients in the fields of food, medicine, and healthcare is often limited by low solubility and poor stability. To enhance the solubility and stability of cinnamaldehyde in aqueous environment, the inclusion technology of β-cyclodextrin and hydroxypropyl β-cyclodextrin was introduced in this study to prepare cinnamaldehyde inclusion complex. The inclusion rate, physicochemical properties, release behavior, stability, and bioavailability were systematically evaluated. The inclusion complex was prepared by solution stirring at a molar ratio of 1:1 and 45℃ with an inclusion rate of 93.47%. Thermal analysis and X-ray diffraction outcomes showed that the inclusion process destroyed the original lattice structure of cinnamaldehyde, causing the crystal form to become amorphous. The *in vitro* release test showed that, under the condition of pH 1.2, the maximum release rate of the inclusion complex was 72.6%, which was lower than the 88.4% of free cinnamaldehyde, and the rate decreased by 14.4% in the initial release stage. After 60 days of accelerated storage, the retention rate of the inclusion complex was 68.5%, significantly higher than the free state's 36.9%, and maintained a retention rate of 80.7% under strong light conditions. The antioxidant test showed that the inclusion complex increased 2,2-diphenyl-1-picrylhydrazyl (DPPH) radical scavenging rate and 2,2′-azino-bis(3-ethylbenzothiazoline-6-sulfonic acid) (ABTS) radical scavenging rate to 90.5% and 93.2%, while the IC_{50} decreased to 0.32 mg/mL and 0.29 mg/mL, respectively. The results indicated that this encapsulation technology could significantly improve the bioavailability, storage stability, and antioxidant activity of cinnamaldehyde, providing an effective pathway for the functional utilization of natural active substances.

Keywords: β-cyclodextrin; hydroxypropyl β-cyclodextrin; cinnamaldehyde; composite material; antioxidant activity.

***Corresponding author:** Yuanyuan Zhang, Cangzhou Medical College, Cangzhou, Hebei 061001, China. Email: zhangyuan_0201@163.com.

Introduction

Natural bioactive compounds have gained increasing attention in food science, pharmaceuticals, and functional health products due to their diverse biological activities and relatively high safety profiles [1, 2]. Among them, cinnamaldehyde, a major active component extracted from cinnamon essential oil, exhibits remarkable antioxidant, antibacterial, anti-inflammatory, and preservative properties [3]. It has been widely explored in food preservation systems, antimicrobial packaging materials, and pharmaceutical formulations. However, its

application in aqueous environments remains limited because of poor water solubility, high volatility, and susceptibility to degradation under light, heat, and pH variations [4, 5]. These physicochemical limitations significantly restrict stability, bioavailability, and functional performance in practical systems.

To overcome these drawbacks, various encapsulation and stabilization technologies have been developed including nanoemulsions, liposomes, polymer nanoparticles, and inclusion complexes [6]. Among these strategies, cyclodextrin-based inclusion technology has shown considerable promise owing to its unique toroidal structure composed of a hydrophobic inner cavity and hydrophilic outer surface [7, 8]. This configuration enables the encapsulation of hydrophobic guest molecules through host–guest interactions, thereby enhancing water solubility, reducing volatility, and improving environmental stability [3, 4]. β-Cyclodextrin (β-CD) is widely used due to its established safety and inclusion capability, while hydroxypropyl-β-cyclodextrin (HP-β-CD), a modified derivative, possesses improved aqueous solubility and stronger complexation ability, making it suitable for constructing high-loading and stable delivery systems [9, 10]. Previous studies have demonstrated that cyclodextrin derivatives can effectively enhance solubility, provide sustained release behavior, and protect bioactive compounds from photodegradation and oxidation [11, 12]. Despite these advances, several challenges remain. Traditional single-cyclodextrin inclusion systems often exhibit limited loading capacity, insufficient structural stability under complex digestive conditions, and suboptimal control over release kinetics. Furthermore, systematic investigations combining dual-cyclodextrin strategies with comprehensive evaluations of release behavior, storage stability, antioxidant activity, and simulated digestion bioavailability are still scarce. Therefore, there is an urgent need to develop an optimized inclusion system that enhances encapsulation efficiency while achieving improved sustained release and digestive stability.

This study constructed a cinnamaldehyde inclusion system synergistically based on β-CD and HP-β-CD using a solution stirring method to optimize inclusion conditions for high encapsulation efficiency, characterize structural and physicochemical changes through differential scanning calorimetry, X-ray diffraction, and Fourier transform infrared spectroscopy, evaluate intramolecular vibrational energy redistribution (IVR) behavior under different pH conditions and analyzing kinetic mechanisms, assess storage and photostability under accelerated conditions, and investigate antioxidant activity and bioavailability using simulated digestion models. By combining dual-cyclodextrin encapsulation techniques with a comprehensive physicochemical and biological assessment, this study developed a more effective stabilization approach for cinnamaldehyde and other hydrophobic bioactive compounds. The results of this research had the potential to enhance the development of superior delivery systems for food preservation, nutraceuticals, and pharmaceuticals, while providing theoretical backing for the advancement of inclusion technology within the realm of functional ingredient engineering.

Materials and methods

Preparation of inclusion compound

Cinnamaldehyde hydroxypropyl/β-cyclodextrin inclusion complex was prepared by solution stirring method. 1.135 g (1 mmol) of β-cyclodextrin was dissolved in 50 mL of ultrapure water at the temperature between 35 - 55℃ on a constant temperature magnetic stirrer until completely dissolved [13, 14]. 0.132 g (1 mmol) cinnamaldehyde was dissolved in 5 mL of ethanol and then mixed with hydroxypropyl/β-cyclodextrin at a molar ratio of 1:1 by slowly dripping into the β-cyclodextrin solution while maintaining a stirring speed of 500 rpm. After 2 hours of reaction with temperature fluctuations

being controlled within ± 0.5℃, the reaction mixture was undergone rotary evaporation by utilizing RE-52AA rotary evaporator (Yarong Biochemical Instrument Factory, Shanghai, China) to eliminate organic solvents and a portion of the moisture. Vacuum freeze-drying was then conducted in FD-1A-50 vacuum freeze dryer (Boyikang Laboratory Instrument Co., Ltd., Beijing, China) to yield a powdered inclusion complex for subsequent evaluation of physical and chemical properties, stability, and bioavailability.

Determination of inclusion rate

50 mg of the complex was mixed with methanol for ultrasonic extraction of free cinnamaldehyde. After filtering through a 0.22 μm polyether sulfone needle filter, the sample was loaded into Agilent 1260 Infinity II high performance liquid chromatography (HPLC) (Agilent Technologies, Santa Clara, CA, USA) to determine the mass of free cinnamaldehyde using C18 chromatographic column (4.6 mm × 250 mm, 5 μm) with mobile phase of methanol water at 70:30 (v/v), flow rate of 1.0 mL/min, detection wavelength of 290 nm, column temperature of 30℃, and injection volume of 20 μL [15]. The inclusion rate was calculated as follows.

$$\rho = \frac{w_z - w_y}{w_z} \times 100\% \quad (1)$$

where w_z was the total mass of cinnamaldehyde in the inclusion reaction. w_y was the measured mass of unencapsulated cinnamaldehyde. ρ was the inclusion rate.

Characterization of physical and chemical properties

The thermal stability was analyzed using NETZSCH DSC 214 Polyma differential scanning calorimetry (NETZSCH, Selb, Germany) with a heating rate of 10℃/min in a nitrogen atmosphere and a testing temperature range from 30 - 300℃. The crystal structure was analyzed using Bruker D8 Advance diffractometer (Bruker, Billerica, MA, USA) with CuK α radiation, voltage 40 kV, current 40 mA, scanning range 5 - 50° (2θ), scanning rate 5°/min. Nicolet iS50 Fourier transform infrared (FTIR) spectrometer (Thermo Fisher Scientific, Waltham, MA, USA) was used to analyze functional group changes with a scanning range of 4,000/cm to 400/cm, a resolution of 4/cm, and 32 scans [16, 17]. The water solubility was determined at 25℃ by adding excess samples to ultrapure water and stirring at a constant speed for 2 hours. The supernatant was then filtered, and the concentration of cinnamaldehyde was determined by using HPLC.

IVR test

The release performance was evaluated under simulated gastric fluid with pH of 1.2 containing 0.32% pepsin and simulated intestinal fluid with pH of 6.8 containing 1% trypsin and 0.5% bile salt. The sample was placed in a dialysis bag with a molecular weight cutoff of 3,500 Da and immersed in a constant temperature water bath at 37 ± 0.5℃ and oscillation speed of 100 rpm containing the release medium. 2 mL of release medium was removed at 0.5, 1, 2, 4, 6, 8, 12, and 24 h and supplemented with an equal volume of fresh medium. After filtering through a membrane, the released cinnamaldehyde content was determined by using HPLC. The kinetic model was then fitted [18].

Stability assessment test

Accelerated storage stability was evaluated under controlled high temperature conditions to simulate long-term storage behavior. 500 mg each of inclusion complex sample and free cinnamaldehyde were sealed in glass vials and stored at 40℃ in a thermostatic water bath for up to 60 days under ambient laboratory humidity conditions. Photostability was tested by placing samples under continuous illumination of 5,000 lx in controlled room temperature condition. pH stabilities were inspected by dispersing samples in buffer solutions at pH 3.0, 7.0, 9.0 and collected them on 0, 10, 20, 30, 45, 60 days. The residual cinnamaldehyde content was determined by HPLC analysis. The retention rate, color difference (ΔE), moisture content variation,

and acid value were calculated to evaluate stability changes under accelerated storage conditions and the protective effect of β-cyclodextrin inclusion on the stability of cinnamaldehyde.

Determination of antioxidant activity

The antioxidant capacity of inclusion complexes and free cinnamaldehyde were evaluated by using DPPH radical scavenging assay. Sample solutions at concentrations of 0.05, 0.1, 0.2, 0.4, 0.8, and 1.0 mg/mL were prepared before mixing with DPPH methanol solution at 25℃ for 30 minutes in the dark. The absorbance at 517 nm was measured using Shimadzu UV-2600 UV–Vis spectrophotometer (Shimadzu, Kyoto, Japan) to calculate the free radical scavenging rate. An ABTS•+ radical scavenging assay was simultaneously conducted by mixing the sample with 2,2'-azino-bis(3-ethylbenzothiazoline-6-sulfonic acid) (ABTS) in a specific ratio, subsequently oxidizing the ABTS with potassium sulfate to generate the ABTS radical cation (ABTS•+), and measuring the change in absorbance at 734 nm.

Determination of bioavailability under simulated digestion conditions

Three *in vitro* simulated digestive system conditions including oral cavity, stomach, and small intestine were employed. In oral stage, the sample was added to a buffer containing 150 U/mL salivary amylase and incubated at 37℃ for 2 minutes. In stomach stage, the pH of the reaction system was adjusted to 2.0, while 250 U/mL gastric protease was added and incubated at 37℃ for 2 hours. In small intestine stage, the pH was adjusted to 7.0, while 200 U/mL pancreatic enzyme and 10 mM bile salt were added and incubated at 37℃ for 2 hours. Samples were taken at the end of each stage. After filtering through a 0.22 μm polyether sulfone filter membrane, the content of cinnamaldehyde was determined by using HPLC to calculate the retention rate and cumulative release rate of each stage.

Data processing

All experiments were conducted concurrently in triplicate with each replicate being entirely independent. The measurement results were presented as the mean ± standard deviation (SD). For each experimental parameter and measurement index, the raw data was first organized and preliminarily calculated using Microsoft Excel 2021 (Microsoft Corporation, Redmond, WA, USA). Origin 2022 (OriginLab Corporation, Northampton, MA, USA) was used to draw the result curves. The dynamic curve fitting in the inclusion rate, solubility, and stability tests were performed using Origin's built-in nonlinear regression module. The release kinetics analysis was performed using the zero-order kinetic models of classical drug release theory, first-order kinetics, Higuchi model, and Korsmeyer–Peppas model for multi model fitting, and the best fitting model was selected based on the coefficient of determination and Akaike Information Criterion (AIC). By incorporating half-life as an assessment metric into the stability decay curve calculations, the study quantified the variations in the degradation rate of cinnamaldehyde under diverse conditions. The calculation of antioxidant test adopted the formula of free radical scavenging rate, and the dose-response relationship curve between scavenging rate and sample concentration. SPSS 26.0 software (IBM Corp., Armonk, NY, USA) was employed for statistical analysis. For parameters that met homogeneity of variance, differences among various treatment groups were assessed using one-way ANOVA followed by Duncan's multiple range test for subsequent pairwise comparisons. For data that did not meet the homogeneity of variance, non-parametric testing methods were used. *P* value less than 0.05 was defined as statistical significance, while *P* value less than 0.01 was defined as extreme significance.

Results and discussion

Package rate analysis

The inclusion rate of cinnamaldehyde hydroxypropyl - β-cyclodextrin complexes

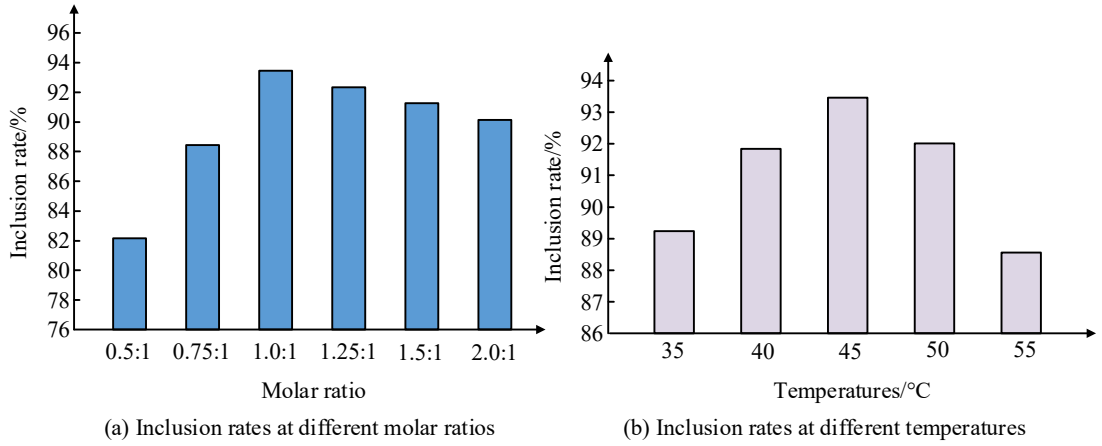

Figure 1. Analysis of package integration rate.

prepared under different molar ratios and reaction conditions demonstrated that, with the increase of molar ratio, the inclusion rate exhibited a pattern where it initially rose and subsequently experienced a minor decline. When the molar ratio was 0.5:1, the inclusion rate was only 82.16%, indicating that the insufficient content of guest molecules led to the underutilization of inclusion sites. When the molar ratio was 1:1, the inclusion rate reached the highest value of 93.47%, and the ratio of host guest molecules was most matched, which could form a relatively stable inclusion structure. When the molar ratios were further increased to 1.5:1 and 2:1, the inclusion rates decreased to 91.28% and 90.15%, respectively, which might be due to the excessive presence of cinnamaldehyde in a free state in the solution that could not enter the cyclodextrin molecular cavity and thus reduce the overall inclusion efficiency (Figure 1a). When the reaction temperature rose from 35℃ to 45℃, the inclusion rate increased from 89.24% to 93.47%, indicating that moderate heating could increase the molecular thermal motion rate, promote the entry of guest molecules into the main molecular cavity, and form stable inclusion complexes. However, when the temperature increased to 50℃ and 55℃, the inclusion rates decreased to 92.02% and 88.56%, respectively, which might be related to the volatilization loss of cinnamaldehyde under high temperature conditions and the weakening of the interaction between host and guest molecules. Additionally, high temperatures might also cause partial damage to the molecular structure of cyclodextrin, thereby reducing the inclusion efficiency (Figure 1b). The results indicated that, under the optimized molar ratio of 1:1 and reaction temperature of 45℃, the inclusion complex with the highest inclusion rate could be obtained.

Characterization of physical and chemical properties

The results showed that pure cinnamaldehyde exhibited an onset temperature of 65.12℃, a melting peak at 74.85℃, and an end temperature of 82.34℃ with a fusion enthalpy of 145.21 J/g, indicating its highly crystalline structure and stable lattice arrangement. Hydroxypropyl - β-cyclodextrin showed an onset temperature of 85.45℃, a peak temperature of 98.12℃, and an end temperature of 105.23℃ with a markedly lower fusion enthalpy of 56.78 J/g, suggesting its relatively amorphous structural characteristics. In contrast, the inclusion complex presented an onset temperature of 78.33℃ and an end temperature of 92.15℃, while the characteristic melting peak of cinnamaldehyde disappeared and no distinct fusion enthalpy was observed. The disappearance of the melting peak and the absence of measurable enthalpy confirmed that cinnamaldehyde was successfully incorporated into the cyclodextrin cavity, leading to disruption

Table 1. Main diffraction peaks and crystallinity.

Sample	Main diffraction peak position (°(2θ))	Peak intensity (a.u.)	FWHM (°)	Crystallinity (%)
Hydroxypropyl-β-cyclodextrin	12.4	220	0.5	78.5
Hydroxypropyl-β-cyclodextrin	18.7	275	0.4	78.5
Hydroxypropyl-β-cyclodextrin	22.8	200	0.6	78.5
Inclusion complex	12.5	140	1.2	42.7
Inclusion complex	18.5	120	1.0	42.7
Inclusion complex	22.5	110	1.1	42.7

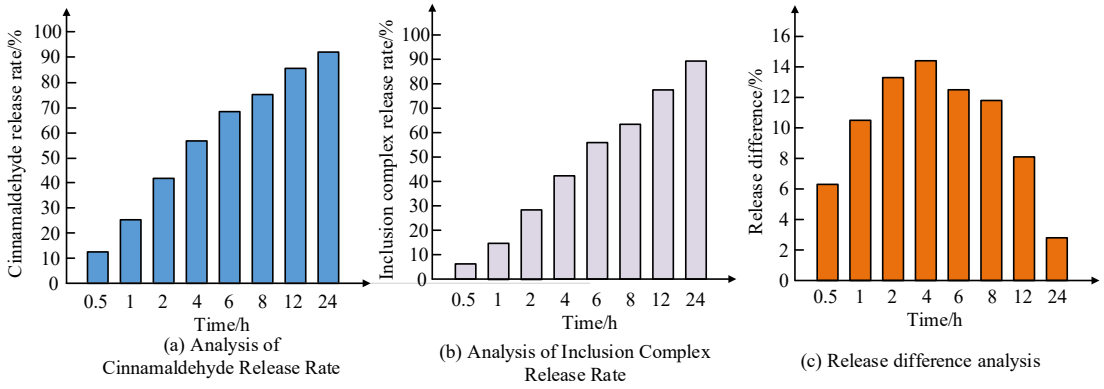

Figure 2. Cumulative release rate at different time points.

of its original crystalline lattice and transformation into an amorphous inclusion structure. To further verify the structural changes of the inclusion complex, X-ray diffraction analysis demonstrated that hydroxypropyl - β-cyclodextrin exhibited distinct and sharp diffraction peaks at 12.4°, 18.7°, and 22.8° with peak intensities of 220, 275, and 200 a.u., respectively, and a crystallinity of 78.5%, indicating its relatively regular crystal structure. The diffraction peak intensity of the inclusion complex at the corresponding positions significantly decreased to 140, 120, and 110 a.u., the half width increased to 1.2°, 1.0°, and 1.1°, the crystallinity decreased to 42.7% and exhibited partial dispersion characteristics (Table 1). This change indicated that, during the inclusion process, cinnamaldehyde molecules entered the cyclodextrin molecule cavity and disrupted the original lattice arrangement, resulting in the amorphous structure of the inclusion complex, further proving the successful occurrence of the inclusion reaction.

IVR performance

The cumulative release profiles of cinnamaldehyde and its inclusion complex showed that the release rate of cinnamaldehyde was relatively fast in the first 6 hours with a cumulative release rate of 68.4%, while the inclusion complex was only 55.9% at the same time point. The maximum difference in release between the two was 14.4% at 4 hours, indicating that hydroxypropyl - β-cyclodextrin inclusion could significantly delay the release process of cinnamaldehyde in the early and middle stages. After 12 hours, the release rates of the two gradually slowed down and approached equilibrium. At 24 hours, the difference in release rates was only 2.8%, indicating that the impact of encapsulation on later release was limited (Figure 2).

Table 2. Release parameters under different pH conditions.

pH	Maximum release rate of cinnamaldehyde (%)	Maximum release rate of inclusion complex (%)	Time to maximum release (h)	Release rate constant k
1.2	88.4	72.6	10	0.152
4.5	90.1	78.4	9	0.168
6.8	92.5	85.7	8	0.192
7.4	93.2	86.9	8	0.198

The release characteristics under various pH conditions showed that, as the pH increased, the maximum release rates of cinnamaldehyde and inclusion complexes both increased, and the time to reach maximum release gradually shortened. Under acidic conditions of pH 1.2, the maximum release rate of the inclusion complex was only 72.6%, significantly lower than the 88.4% of free cinnamaldehyde, indicating that the inclusion structure could effectively inhibit the rapid release of cinnamaldehyde in acidic environments. The release rate constant k increased with increasing pH, especially under pH 6.8 and pH 7.4 with significantly accelerated release process (Table 2), which might be related to the partial dissociation of the inclusion complex structure and the increased solubility of cinnamaldehyde under alkaline conditions. To reveal the release mechanism, the experimental data were fitted using zero-order, first-order, Higuchi, and Korsmeyer–Peppas kinetic models. The fitting results showed that the Korsmeyer–Peppas model provided the best correlation with R^2 values of 0.981 for free cinnamaldehyde and 0.992 for the inclusion complex. The corresponding release rate constants were 0.48 and 0.39, respectively, indicating that the inclusion complex exhibited a slower release rate compared to the free form. The release mechanism index (n) of the inclusion complex was 0.45, suggesting that the release process was predominantly governed by Fickian diffusion. The Higuchi model also demonstrated good fitting performance with R^2 values of 0.968 and 0.987 for the free and inclusion forms, respectively, further confirming the role of diffusion in controlling drug release. In contrast, the zero-order model showed relatively lower fitting accuracy with R^2 of 0.894 for free cinnamaldehyde and 0.923 for the inclusion complex, indicating that the release process did not follow an ideal constant-rate pattern.

Stability evaluation

The stability of cinnamaldehyde and its inclusion complex under accelerated storage conditions demonstrated that, during the 60 day accelerated storage process, the retention rate of cinnamaldehyde decreased from 100% to 36.9%, while the retention rate of the inclusion complex remained at 68.5% under the same conditions, significantly higher than that of free cinnamaldehyde, revealing that the inclusion structure had a significant protective effect on the active ingredient. The color difference ΔE gradually increased with storage time with cinnamaldehyde reaching 6.87 at 60 days. However, the color difference of the inclusion complex changed relatively slowly, indicating that the inclusion complex had a good effect on maintaining color stability during storage. The changes in moisture content and acid value showed an upward trend in the later stage of storage with cinnamaldehyde acid value increasing from 0.25 to 0.79 and inclusion complex increasing to 0.64, indicating that inclusion could effectively slow down the process of lipid oxidation (Table 3). The stability test outcomes under varying lighting conditions showed that the light intensity significantly influenced the stability of both cinnamaldehyde and its inclusion complexes. The stronger the light intensity, the more obvious the decrease in retention rate, and the significant increase in color difference ΔE. Under strong light conditions, the retention rate of cinnamaldehyde was only 55.2%, while the inclusion complex still had 80.7%, indicating that the inclusion complex

Table 3. Stability under accelerated storage conditions.

Storage time (d)	Cinnamaldehyde retention (%)	Inclusion complex retention (%)	Color difference (ΔE)	Moisture content change (%)	Acid value change (mgKOH/g)
0	100	100	0	0	0.25
10	85.6	94.8	1.52	0.12	0.33
20	71.3	89.1	2.85	0.21	0.42
30	60.2	82.7	3.98	0.28	0.53
45	48.5	75.3	5.34	0.35	0.64
60	36.9	68.5	6.87	0.41	0.79

Table 4. Stability under different lighting conditions.

Light condition	Cinnamaldehyde retention (%)	Inclusion complex retention (%)	Color difference (ΔE)	Moisture content change (%)	Acid value change (mgKOH/g)
Dark	95.6	98.2	1.02	0.12	0.31
Low light	78.4	90.5	3.46	0.24	0.48
Strong light	55.2	80.7	6.78	0.38	0.72

was significantly better than cinnamaldehyde in terms of photostability (Table 4). The trends of changes in moisture content and acid value were consistent with the retention rate. Light exposure intensified the water evaporation and oxidation reactions of the sample, while the light blocking and shielding effects of the inclusion complex structure effectively reduced the magnitude of these changes, thereby delaying the degradation process of cinnamaldehyde under light conditions.

Comparison of antioxidant activity

The DPPH radical scavenging activity of cinnamaldehyde and its inclusion complex increased with increasing concentrations from 0.05 – 1.0 mg/mL. At 1.0 mg/mL, the scavenging rate of free cinnamaldehyde reached 82.6%, whereas the inclusion complex achieved 90.5%, representing an increase of 7.9%. Under low concentration of 0.05 mg/mL, the difference was more pronounced with scavenging rates of 20.4% and 28.9% for the free and inclusion forms, respectively. Kinetic analysis showed that the reaction rate constant k of the inclusion complex was 0.112/min, which was higher than that of free cinnamaldehyde's 0.085/min, indicating accelerated radical scavenging kinetics after encapsulation. The IC_{50} decreased from 0.46 mg/mL to 0.32 mg/mL, demonstrating enhanced antioxidant potency. In addition, the antioxidant capacity (TEAC) increased from 1.25 to 1.78 mmol/L, confirming improved electron-donating capacity. A similar trend was observed in the ABTS radical scavenging assay. At 1.0 mg/mL, the scavenging rate of the inclusion complex reached 93.2%, significantly higher than 86.4% for free cinnamaldehyde. During the initial reaction stage (5 min), the inclusion complex exhibited a higher scavenging rate of 39.2% compared to the free form of 30.8%, indicating faster initial reaction kinetics. The kinetic rate constant k increased from 0.091/min to 0.119/min after encapsulation, while the IC_{50} decreased from 0.41 mg/mL to 0.29 mg/mL. The TEAC value of the inclusion complex reached 1.92 mmol/L, higher than 1.38 mmol/L of the free form, demonstrating superior antioxidant efficiency.

Analysis of bioavailability under simulated digestion conditions

The bioavailability under simulated digestion conditions showed that, under simulated oral, gastric, small intestine digestion conditions, the

Table 5. Bioaccumulation analysis.

Sample	Free form			Inclusion complex		
Phase	**Oral**	**Gastric**	**Intestinal**	**Oral**	**Gastric**	**Intestinal**
Retention at end of phase (%)	96.3	68.7	42.5	98.1	83.4	65.2
Cumulative release rate (%)	2.7	20.5	40.1	1.2	10.6	27.5
Cumulative degradation rate (%)	1.0	10.8	17.4	0.7	6.0	7.3
First-order rate constant k (/min)	0.006	0.018	0.022	0.004	0.01	0.015
Half-life $t_{1/2}$ (min)	115	38	31	173	69	46
Higuchi slope (mg/L·$min^{0.5}$)	0.35	1.12	1.45	0.28	0.78	1.02
Peppas index (n)	0.48	0.53	0.56	0.43	0.45	0.46
Phase AUC (concentration–time) (mg·min/L)	85	410	690	62	290	520
Phase antioxidant capacity retention (TEAC) (mmol/L)	1.18	0.98	0.86	1.62	1.51	1.44

Note: Oral phase: 2 min. Gastric phase: 120 min. Intestinal phase: 120 min. All at 37℃.

inclusion complex maintained higher retention rates of active ingredients and lower degradation rates at all stages, demonstrating overall superior bioavailability potential. During the oral stage, the retention rate of the inclusion complex reached 98.1%, slightly higher than 96.3% in the free state, and the degradation rate was only 0.7%, indicating good stability upon initial contact. During the gastric stage, free cinnamaldehyde decreased to 68.7% in acidic and enzymatic conditions, while the inclusion complex still had a retention rate of 83.4% and a degradation rate of only 6.0%, indicating that inclusion significantly delayed the loss of gastric phase activity. In the small intestine stage, the free state retention rate further decreased to 42.5%, while the inclusion complex remained at 65.2%, indicating that it could provide a higher effective concentration at the main absorption site. Dynamics analysis showed that the first-order rate constant of the inclusion complex was lower than that of the free state at each stage, the half-life was prolonged, the Higuchi slope and Peppas index were slightly lower, indicating that the release was regulated by a combination of diffusion and matrix degradation, which was consistent with the sustained-release characteristics and helped to reduce premature release in the gastric phase and optimize intestinal phase supply. The AUC results further confirmed that the concentration-time integral of the inclusion complex in both gastric and small intestinal phases was notably higher than that in the free state, indicating a greater cumulative available amount within the absorption window. In terms of functional preservation, the antioxidant capacity (TEAC) of the inclusion complex was higher than that of the free state at all stages, especially in the oral stage, which was 0.44 mmol/L higher, indicating that structural protection effectively reduced activity attenuation during digestion (Table 5). The results suggested that the β-CD and HP-β-CD inclusion technology not only improved the stability of cinnamaldehyde in the digestive environment but also enhanced its bioavailability by controlling release and reducing degradation.

Conclusion

An inclusion system based on β-cyclodextrin and hydroxypropyl - β-cyclodextrin was successfully constructed to overcome the limitations of cinnamaldehyde in aqueous environments. Structural characterization confirmed the formation of a stable host–guest inclusion complex, accompanied by disruption of the original crystalline structure and transformation toward an amorphous state. The encapsulation system effectively regulated the release behavior of cinnamaldehyde under simulated digestive conditions, demonstrating sustained-release characteristics and enhanced resistance to rapid degradation in acidic environments. Stability evaluation indicated that the inclusion complex

provided significant protection against thermal and photodegradation, thereby improving storage performance. Furthermore, the antioxidant capacity of cinnamaldehyde was enhanced after encapsulation with improved radical scavenging efficiency and reaction kinetics. Simulated digestion analysis demonstrated improved retention and controlled release throughout the gastrointestinal phases, suggesting enhanced bioavailability potential. Overall, the β-CD and HP-β-CD dual inclusion strategy represented an effective approach for improving physicochemical stability, controlled release performance, and functional activity of hydrophobic bioactive compounds. Future studies may focus on evaluating performance in complex food or pharmaceutical matrices and investigate long-term metabolic behavior *in vivo*.

References

1. Kang L, Yue K, Ma C. 2024. Mediating Zn ions migration behavior *via* β-cyclodextrin modified carbon nanotube film for high-performance Zn anodes. Nano Lett. 24(14):1-8.
2. Ao S, Yu X, Wang X. 2025. Sodium ion diffusion behavior in multiple open/closed pore ratios of novel β-cyclodextrin-derived hard carbon anode materials. Nano Lett. 25(4):1314-1321.
3. Zhang M, Wen Y, Zhang Z. 2024. Long *in vitro* circulating nanomicelles formed by sharp-contrast Janus star polymers derived from β-cyclodextrin grafted with lipids and polyzwitterions. Nano Today. 59:102511.
4. Wu H, Wang Y, Tang C. 2023. High-efficiency gold recovery by additive-induced supramolecular polymerization of β-cyclodextrin. Nat Commun. 14(1):14-25.
5. Cheng Q, Ma X, Zhou X. 2024. Polymerization based on modified β-cyclodextrin achieves efficient phosphorescence energy transfer for anti-counterfeiting. Small. 20(17):11-24.
6. Yao T, Chen H, Luo Y. 2024. Preparation of β-cyclodextrin-reduced graphene oxide aerogel and its application for adsorption of herbicides. J Clean Prod. 468:143109.
7. Zhang F, Xu H, Li T, Li X, Zhou D, Wu C, *et al*. 2024. Exploring the binding process of lutein with hydroxypropyl-β-cyclodextrin: Multispectral and molecular simulation study. Food Hydrocoll. 156:110293.
8. Huang C, Wang Y, Qiang J. 2025. Inclusion of α-linolenic acid ethyl ester in flaxseed oil with β-cyclodextrin by hydrogen bonding. Food Chem. 472:142860.
9. Ozelcaglayan ED, Parker W. 2023. β-cyclodextrin functionalized adsorbents for removal of organic micropollutants from water. Chemosphere. 320:137964.
10. Li N, Yang X, Zuo S. 2023. Interfacially polymerized β-cyclodextrin film for rapid removal of organic dyes. Macromol Rapid Commun. 44(15):2300064.
11. Ishak MAI, Aun TT, Sidek N. 2024. An enantioselective study of β-cyclodextrin and ionic liquid-β-cyclodextrin towards propranolol enantiomers by molecular dynamic simulations. J Comput Chem. 45(16):1329-1351.
12. Huang C, Zhang X, Li X. 2024. β-cyclodextrin enhanced bioavailability of petroleum hydrocarbons in industrially contaminated soil: A phytoremediation field study. Int J Phytoremediation. 26(12-14):2348-2355.
13. Yalin W, Xinyun T, Yin H. 2025. Novel fabrication of hydroxypropyl-β-cyclodextrin functionalized zein protein nanoparticles co-encapsulated with biomolecules to attenuate pregnancy-induced hypertension. J Biomater Appl. 40(1):118-134.
14. Sun Y, Jiang L, Chen Y. 2024. *In situ* crosslink polymerization induced long-lived multicolor supramolecular hydrogel based on modified β-cyclodextrin. Chin Chem Lett. 35(2):374-379.
15. Li Y, Chen X, Li H. 2024. Preparation and application in the paper protection of carboxymethyl cellulose grafted with β-cyclodextrin. Nord Pulp Pap Res J. 39(3):517-526.
16. Doan VTH, Katsuki J, Takano S. 2023. Determining the critical quality attribute for the delivery of α-mangostin by β-cyclodextrin-based nanoparticles in cancer treatment. Polym J. 55(12):1367-1378.
17. Wang J, Lin ZW, Dichtel WR. 2024. Perfluoroalkyl acid adsorption by styrenic β-cyclodextrin polymers, anion-exchange resins, and activated carbon is inhibited by matrix constituents. Water Res. 260:121897.
18. Wang S, Wang M, Wu H, Sun X, Dong Z, Peng W, *et al*. 2025. Microwave-assisted synthesis of a β-cyclodextrin/TEMPO-oxidized cellulose/Fe_3O_4 adsorbent for Pb and Cu remediation in soil. J Clean Prod. 495:145100.